LEGIBILITY NOTICE

A major purpose of the Technical Information Center is to provide the broadest dissemination possible of information contained in DOE's Research and Development Reports to business, industry, the academic community, and federal, state and local governments.

Although a small portion of this report is not reproducible, it is being made available to expedite the availability of information on the research discussed herein.

LA-UR -87-3035

CONF-8709110 --1

Los Alamos National Laboratory is operated by the University of California for the United States Department of Energy under contract W-7405-ENG-36

TITLE THE GENERATION AND SUPPRESSION OF SYNCHROTRON SIDEBANDS

LA--UR--87-3035

DE88 000532

AUTHOR(S): R. W. Warren and J. C. Goldstein

SUBMITTED TO Ninth International FEL Conference, Williamsburg, Virginia
September 14-18, 1987

DISCLAIMER

MASTER

Los Alamos Los Alamos National Laboratory
Los Alamos, New Mexico 87545

THE GENERATION AND SUPPRESSION OF SYNCHROTRON SIDEBANDS*

Roger W. WARREN (H825) and John C. GOLDSTEIN

Los Alamos National Laboratory, Los Alamos, NM 87545

Computer simulations of FEL lasing differ in the degree to which they approximate real experiments. One of the FEL codes used extensively at Los Alamos takes account of the features of each electron micropulse and follows the growth and saturation of the optical micropulse. With no additional adjustments, this code displays the development of sidebands and demonstrates their control when optical filters of various kinds are used. Other codes that do not include a description of the micropulse do not automatically display sidebands but need to have artificial noise of some kind added. This is not unexpected because sidebands are generated by an FEL instability; instabilities, in general, need some kind of initiating disturbance.

In this paper we have

(1) identified the disturbance that triggers the instability in the pulse code,
(2) discovered a practical way to suppress the instability without using filters,
(3) compared these results with experiments, and
(4) discussed these findings.

1. Introduction

The longitudinal oscillation of electrons in the ponderomotive potential well of a free-electron (FEL) laser is an unstable motion that can grow to large amplitude, ejecting electrons from the bucket and generating a strong sideband structure to the

*Work performed under the auspices of the U.S. Dept. of Energy and supported by the U.S. Army Strategic Defense Commande.

optical spectrum [1-8]. For uniform wigglers the consequence can be an enhanced extraction efficiency, but for long, tapered wigglers [9-11] the inevitable result is a serious reduction in efficiency and an unattractively wide spectral output. It has been shown theoretically [9,11] that both of these bad effects can be greatly reduced by using optical filters inside the cavity resonator. Experiments [12,13] have successfully demonstrated the reduction of sidebands using filters but, so far, at the expense of reduced efficiency. The major requirements on the filter are a sharp discrimination between wanted and unwanted light and the ability to withstand physical destruction by the very high optical fields inside a typical FEL cavity. If the filter has a narrow passband, there are additional problems during the growth from small signal to saturation because of the frequency chirp demonstrated by most wigglers during startup.

Like any instability, the synchrotron instability depends upon some perturbing event to start it growing. There are two basically different kinds of initial perturbations, boundary and internal. Their nature can be illustrated by discussing the computer simulations that employ them. One kind of simulation [8,14] models the complete electron and optical micropulse structure and demonstrates the development of the instability at the beginning and, sometimes, the end of the micropulse, i.e., at its boundaries, in a natural way without any special assumptions. Simulations [15] using periodic boundary conditions, on the other hand, model only the central part of a micropulse and would not trigger the instability at all except for the introduction of some kind of artificial optical noise.

2. Discussion

Because of the disadvantages of using optical filters inside the optical cavity at high power levels, we are interested in exploring the possibility of using other

techniques to suppress the generation of sidebands. Any successful control technique must be able to reduce the magnitude of the perturbation that generates the sidebands or to reduce its growth rate. We obviously need to know a great deal about the perturbations and how they grow. Accordingly, we pose four fundamental questions about the perturbations:

- What are the sources of the internal noise in a real experiment?
- How does the internal noise compare in strength with the boundary noise, i.e., the perturbation caused by the initiation and end of each micropulse?
- Are there ways to suppress either or both?
- Can these techniques be put into practice?

We answer these questions in the following sections by describing how lasing grows and by discussing the generation of sidebands, the influence of optical filters, the effects of detuning, and the effects and possible sources of fluctuations of certain parameters. Special simulations will be performed to test special kinds of perturbations and suggested methods of sideband control. These steps are largely descriptive, but are based on a wealth of calculations accumulated over several years. Whenever particularly crucial assertions are made, the results of the simulations on which they are based will be presented. This discussion is organized into four parts: a brief description of the simulations; a description, with examples, of the process by which sidebands develop; a comparison of the simulations with experiment; a discussions of internal noise sources.

2.1. Simulations

The simulations to be presented in this paper are discussed in detail elsewhere [7,14,16]. They are one-dimensional calculations that model one complete optical micropulse undergoing interactions with a string of electron micropulses. The optical micropulse is described in terms of its amplitude and its phase with respect to a standard reference signal. Its frequency spectrum is determined by performing an appropriate transform of the pulse. Lasing is normally initiated from spontaneous emission generated by electron shot noise with zero initial optical density. Alternatively, a weak monochromatic signal is sometimes used when fluctuations would obscure some effect of interest. Most of the features of the lasing do not depend on the details of its initiation.

The electron micropulses can be tailored in various ways to include fluctuations or noise, for example, by altering their amplitude, energy, or timing in the macropulse or within a micropulse. A series of calculations has been performed with different variations of this sort to model internal noise sources. The standard calculation, however, includes no fluctuations of any kind. It uses the following parameters for the electron micropulse: energy, 20 MeV; peak current, 40 A; shape, parabolic; width 20 ps; energy spread, zero; emittance, zero. The wiggler has the following properties: length, 1 m; peak field strength, 3 kG; wavelength, 2.7 cm (constant). The optical cavity is 7 m long and the light generated is at a wavelength of 10 μm with a Rayleigh length of 0.7 m.

With these parameters, the laser produces a small signal gain of ~80% and a saturated gain of 3% (as determined by cavity losses), characteristics similar to those of the FEL oscillator used with a uniform wiggler at Los Alamos. The Los Alamos system actually has a larger peak current but also has significant energy spread and emittance. We have chosen the standard system to be without energy spread or

emittance to simplify the calculations and with an unnaturally low current to give the experimental values of gain and efficiency. We do not believe that this simplification has important consequences to the development of sidebands.

2.2. How sidebands grow in response to boundary noise

2.2.1. Typical micropulse shapes and spectra during growth

Figs. 1A-D show the shape and amplitude of the optical micropulse resulting from the standard calculation after the passage of, respectively, 25, 75, 125, and 200 electron micropulses. Figs. 2A-D show the corresponding spectra. Fig. 3 shows the rapid growth in extraction efficiency that occurs until an initial saturation sets in around pass 100. Further slow growth occurs between pass 100 and pass 200. This is also the time when strong oscillations in amplitude and phase grow at the front of the micropulse.

Three important observations can be made from these figures:

(1) Sideband oscillations are apparent in the simulations only after the initial saturation is reached.

(2) The oscillations start only at the beginning of the micropulse.

(3) The oscillations slowly grow in amplitude and spread to later times in the pulse.

2.2.2. Use of an optical filter to control the modulation

An ideally sharp optical filter has been used in simulations to suppress the sideband growth. This filter contributes no phase shift to the optical wave, but does completely absorb all components with wavelengths longer than a cutoff wavelength that is somewhat longer than the main line of the spectrum. This filter can

that is somewhat longer than the main line of the spectrum. This filter can successfully suppress the sidebands, generating a modulation-free pulse and a narrow spectrum. Its performance, however, is considerably more complicated than might be expected and depends critically upon the choice of cutoff wavelength.

If the cutoff occurs at a wavelength only very slightly longer than the wavelength of maximum small signal gain, the optical power is limited to the first plateau of fig. 3 and no chirping or sidebands occur. This behavior is shown by curve A of fig. 3. If, on the other hand, the filter's critical wavelength is a few percent longer, chirp occurs, apparently through the complex sideband-mediated process [7]. In this process the following steps occur: a sideband is developed on the long-wavelength side of the original line; because of saturation of the laser, the gain at the sideband exceeds the gain at the original wavelength; the sideband grows rapidly, becoming the strongest line, while the original line becomes insignificant. This quantized step to longer wavelengths repeats itself until the wavelength reaches the peak of the saturated gain curve (where permanent sidebands then develop) or until a limit is imposed by the filter. During these chirp steps, the wiggler's efficiency and the optical power level increase. Fig. 4 shows a simulation (under somewhat different conditions than those shown in fig. 3) where we have used the filter that allows a moderate chirp for curve A; curve B is without a filter. The abrupt steps in efficiency for curve A near pass 100 correspond to the chirp steps.

2.2 3. Detuning curve

Curves like those shown in fig. 3 were prepared with a variety of cavity lengths. Fig. 5 is a plot of the efficiencies achieved on these curves versus detuning. Two different kinds of efficiency are plotted, the efficiency reached at early

range of detunings where the efficiency at early saturation is relatively independent of detuning.

At this point we have discovered three ways to assure that sidebands are absent:

(1) Pay attention only to the early part of the macropulse where sidebands have not yet had a chance to grow.

(2) Suppress the sidebands with an optical filter.

(3) Detune the cavity sufficiently.

A fourth technique is to lase weakly at a low electron beam current or with large cavity losses. This approach is of little interest because of its low efficiency. The first three techniques, however, produce the same higher efficiency and the same optical power, but the ways in which they avoid sidebands are quite different. The effect of a filter is to smooth out the modulation in the optical micropulse as it forms. The absence of sidebands in the early stage of growth is also easy to understand: the sideband frequency depends upon optical power [7,8]. Because of this dependence, any sideband that is generated during the rapid growth phase continually shifts its frequency in response to the growing power. Thus, no sustained growth can occur at any one frequency.

2.2.4. How detuning works to supress sidebands

Detuning is more complex. A special simulation was performed to explore its workings. This simulation was like those described above except that the detuning was changed from zero to -30 μm after strong modulation had developed (at pass 433). The choice of -30 μm was made because fig. 5 indicates that no sidebands should be found there. Following the introduction of detuning, the efficiency slowly dropped (by a factor of about 4), and the sidebands slowly disappeared. The

disappearance of the sidebands can be understood by examining figs. 6A-D and 7A-D, which show the shapes of the optical micropulse at passes 425, 625, 650, and 700 as well as their spectra. In the interval from pass 433 to 625, the very strong modulation produced by the instability is shifted to the leading edge of the pulse and, in subsequent passes, slides forward further until after pass 700 it is completely absent. The rate of slide is 60 μm/pass, i.e., exactly the rate that one would expect for a 30-μm detuning.

If one carefully examines the pulse shapes for zero detuning, for example in figs. 1A-D, it is clear that pulse modulation first occurs at the leading edge of the micropulse and then grows by increasing its amplitude and by creeping through the pulse to later times. A rough measurement from these figures shows that the creep rate is about 20 μm/pass. The creep rate will obviously depend on experimental parameters, and we believe it will increase rapidly with current. The creep rate is important because a kind of competition exists in which the modulation moves to later times at the creep rate but to earlier times at the slide rate set by the detuning. If the slide rate dominates, the modulation introduced at the beginning of a pulse slides off that end of the pulse and sidebands are completely suppressed; otherwise, the modulation creeps into the pulse until the whole pulse is modulated. This interpretation of the role of the creep rate is reinforced by fig. 5, which shows, in agreement with our arguments, that detunings greater than about 20 μm eliminate sidebands.

Slide has a second important effect. If a perturbation were somehow introduced in the center or end of a micropulse instead of at the beginning, the modulation that results would slide across the width of the pulse towards its beginning. While the modulation slides, it normally grows in amplitude. Again a competition exists. If the modulation starts out weak enough and if it grows slowly, the limited time that it has to grow will constrain its final amplitude to a low value.

2.3. Comparison with experiment

A major prediction that follows from the discussions presented above is that the leading edge of a micropulse acts as a very strong trigger for sideband generation but that sufficient detuning, for example to point A on fig. 5, should completely suppress this instability without a loss in efficiency over that sustained by using an optical filter. We have considerable confidence in simulations such as those described here for they have, in most cases, been in good agreement with experiments. In particular, they give correctly the magnitude and frequencies of the sidebands and have predicted, in agreement with observations, that sidebands enhance the efficiency of uniform wigglers.

The simulations [12,17], however, do not agree with the shape or the details of experimentally determined detuning curves. Fig. 8 compares the shapes. Sidebands are observed for all detunings in the experimental curve, although their amplitude and complexity drop steadily as detuning increases. In contrast, sidebands are present only in the central peak of the simulated curve. Thus complete suppression of sidebands at moderate detuning is a feature of the simulations but not the experiments.

2.4. Internal noise sources

In the discussions presented above, we have emphasized the importance of the perturbation caused by the pulse's leading edge and have ignored the possible contribution of perturbations inside the pulse. If internal sources exist, their perturbations will grow as they slide across the micropulse towards its beginning. If the strength of the initial perturbation, or its growth rate, is large enough, the

modulation and the sideband structure will become significant. On the other hand, because the perturbation can only grow during the short time that it slides across the micropulse, it must be a very strong perturbation. The strategy of detuning will reduce the growth of the perturbation but cannot completely quench it.

We can imagine at least four noise sources that might be the kind we seek:

(1) Unavoidable shot noise in the electron beam or photon quantum noise.

(2) Boundary noise occurring at the *end* of a micropulse.

(3) Micropulse timing fluctuations. If the electron micropulse shows large fluctuations in timing (several picoseconds) during a macropulse, its steep front edge will occasionally overlap the interior part of the optical micropulse, causing boundary noise and generating synchrotron modulation there. In experiments, we have observed [18] timing fluctuations of this kind and of this magnitude.

(4) Fluctuations of other properties of the electron beam micropulse that affect its interaction with the light and can, therefore, act as a noise source. These include fluctuations in current, energy, aiming, and focus.

To test source 1, we have purposely introduced noise into the electron current and the light that is used to initiate lasing. We find that detuning normally "flushes" this noise off the front of the micropulse before it can attain an appreciable magnitude. The level of these noise sources must be very much in excess of realistic levels before it has any impact upon the shape of a micropulse or its spectrum.

For source 2, we have occasionally observed modulation growing at the end of a micropulse, but it is relatively rare, requiring a current much higher than that used in the experiment described above.

We have performed a series of special simulations to test source 3. We have allowed the timing of the individual micropulses to vary either randomly or in a sinusoidal fashion with an amplitude of 4 ps. The random fluctuations produced no sidebands when the detuning was -30 μm. The sinusoidal fluctuation with a period

For source 2, we have occasionally observed modulation growing at the end of a micropulse, but it is relatively rare, requiring a current much higher than that used in the experiment described above.

We have performed a series of special simulations to test source 3. We have allowed the timing of the individual micropulses to vary either randomly or in a sinusoidal fashion with an amplitude of 4 ps. The random fluctuations produced no sidebands when the detuning was -30 μm. The sinusoidal fluctuation with a period of 217 passes (10 μs) was chosen to model real experimental fluctuations [18]. Very weak sidebands were generated, but the current had to be increased from 40 to 80 A before the sidebands became strong. Figs. 9A-H show the micropulse's shape at various stages in this 217-pass cycle. We have not yet examined fluctuations with other periods or amplitudes.

Fluctuations in timing are equivalent to fluctuations in detuning. Thus, this kind of periodic timing variation sweeps the effective detuning around -30 μm from about -20 to -40 μm. During the short interval when the detuning is -20 μm, fig. 9A, sidebands are generated strongly, whereas they decay away when the detuning is significantly larger. In this way, relatively strong sidebands are generated at detunings for which they would not be seen at all in the absence of fluctuations.

A careful reader may have noted that a sweep of detuning from -40 to -20 μm does not reach into the region of fig. 5 where sidebands are generated, seemingly contradicting our assertions. Note, however, that fig. 5 is appropriate for a current of 40 A, a current where the modulation in timing was unsuccessful in generating strong sidebands. At 80 A the detuning curve has presumably changed sufficiently so that sidebands are generated at a detuning of -20 μm.

Source 4 (current, energy, or focus variations within a micropulse) also appears likely to generate strong perturbations of the kind required. In attempting to

center of each micropulse drops to a value 10% below its value on the wings of the micropulse. The simulation shows that, contrary to our expectations, the flushing action caused by detuning completely suppresses this very strong perturbation.

We next allowed the current in a micropulse to undergo modest sinusoidal fluctuations in amplitude with a period of 10 μs. No sidebands were generated. As a last effort, we allowed the current in a micropulse to have closely spaced random fluctuations in amplitude of 10%. This modification did generate sidebands, but the perturbation appears to be unrealistic unless there is some kind of plasma oscillation present that causes the rapid fluctuations.

3. Conclusions

We will first attempt to answer the questions posed in the introduction.

- We believe that the major source of noise internal to a micropulse is the variation in the timing of the micropulse.
- To compare the noise strengths, the noise generated by the leading edge of the electron micropulse is the major noise source. It can easily and completely be suppressed by detuning so that only internal noise remains.
- A combination of strategies can be used to reduce the strengths and consequences of both kinds of noise. The main ones are listed below:
  - Detune the optical cavity.
  - Eliminate the variations in timing of the micropulse.
  - Eliminate wake-field effects.
- Detuning can easily be accomplished in practice. Reducing timing fluctuations and wake-field effects has been a continuing effort at Los Alamos [21,22]. Further progress can be expected.

The advantages to be gained by eliminating sidebands without using optical filters are important, especially for high-power FELs. Detuning appears to be a promising technique to accomplish this goal for uniform and various kinds of tapered wigglers. Modifications to the Los Alamos experiment are being planned to reduce timing variations as well as wake-field effects. More simulations will be performed to clarify the role played by the various noise sources and, in particular, to investigate the degree to which timing fluctuations must be reduced to make detuning a useful strategy.

4. Acknowledgments

The ideas presented in this paper have evolved over a period of years. We thank many members of the staff at Los Alamos for fruitful discussions.

References

[1] N. M. Kroll and M. N. Rosenbluth, "Sideband Instability in Trapped Particle Free-Electron Lasers," in Free-Electron Generators of Coherent Radiation, Physics of Quantum Electronics 7, S. F. Jacobs, H. S. Pilloff, M. Sargent III, M. O. Scully, and R. Spitzer, eds. (Addison-Wesley, Reading, MA, 1980), 147-174.

[2] N. M. Kroll, P. L. Morton, and M. N. Rosenbluth, "Free-Electron Lasers with Variable Parameter Wigglers," IEEE J. Quant. Electron. 17, 1436-1468 (1981).

[3] H. Al-Abawi, J. K. McIver, G. T. Moore, and M. O. Scully, "Pulse Propagation in the Tapered Wiggler," in Free-Electron Generators of Coherent Radiation, Physics of Quantum Electronics 8, S. F. Jacobs, G. T. Moore, H. S. Pilloff, M.

Sargent III, M. O. Scully, and R. Spitzer, eds. (Addison-Wesley, Reading, MA 1982), 415-456.

[4] W. B. Colson, "Optical Pulse Evolution in the Stanford Free-Electron Laser and in a Tapered Wiggler," in Free-Electron Generators of Coherent Radiation, Physics of Quantum Electronics 8, S. F. Jacobs, G. T. Moore, H. S. Pilloff, M. Sargent III, M. O. Scully, and R. Spitzer, eds. (Addison-Wesley, 1982), 457-488.

[5] J. C. Goldstein and W. B. Colson, "Pulse Propagation in Free-Electron Lasers with a Tapered Undulator," in Proceedings of the International Conference on Lasers 1981, C. B. Collins ed., (STS Press, 1982), 93-99.

[6] J. C. Goldstein and W. B. Colson, "Control of Optical Pulse Modulation due to the Sideband Instability in Free-Electron Lasers," in Proceedings of International Conference on Lasers 1982, R. C. Powell, ed. (STS Press, McLean, VA, 1983), 218-225.

[7] J. C. Goldstein, "Evolution of Long Pulses in a Tapered Wiggler Free-Electron Laser," in Free Electron Generators of Coherent Radiation, C. A. Brau, S. F. Jacobs, and M. O. Scully, eds., SPIE 453, 2-10 (1984).

[8] W. B. Colson and R. A. Freedman, "Synchrotron Instability for Long Pulses in Free-Electron Laser Oscillators," Opt. Commun. 46, 37-42 (1983).

[9] D. C. Quimby, J. M. Slater, and J. P. Wilcoxon, "Sideband Suppression in Free-Electron Lasers With Multiple Synchrotron Periods," IEEE J. Quant. Electron. 21 (7), 979 (1985).

[10] H. Takeda, B. D. McVey, and J. C. Goldstein, "Theoretical Study of a High Extraction Efficiency Undulator for a Free-Electron Laser Oscillator," Proc. 8th Int. FEL Conference, Glasgow, Scotland, September 1986, to be published in Nucl. Instr. and Meth. in Phys. Research.

[11] R. L. Tokar, B. D. McVey, and J. C. Goldstein, "Sideband Suppression in Free-Electron Lasers using a Grating Rhomb," these proceedings.

[12] R. W. Warren, B. E. Newnam, and J. C. Goldstein, "Raman Spectra and the Los Alamos Free-Electron Laser," IEEE J. Quant. Electron. 21 (7), 882-888, (1985).

[13] J. C. Goldstein, B. E. Newnam, and R. W. Warren, "Sideband Suppression by and Intracavity Optical Filter in the Los Alamos Free-Electron Laser Oscillator," these proceedings.

[14] W. B. Colson and S. K. Ride, "The Free-Electron Laser: Maxwell's Equations Driven by Single-Particle Currents," in Free-Electron Generators of Coherent Radiation, S. F. Jacobs, ed., 1980, 377.

[15] W. B. Colson, "Chaotic Optical Modes in Free-Electron Lasers," in Free-Electron Generators of Coherent Radiation, C. A. Brau, ed., 1984, 290-296.

[16] W. B. Colson and A. Renieri, "Pulse Propagation in Free-Electron Lasers," in Proc. Bendor Free-Electron Laser Conference, J. Phys., (Paris) 11-28 (1983).

[17] J. C. Goldstein, B. E. Newnam, R. W. Warren, and R. L. Sheffield, "Comparison of the Results of Theoretical Calculations with Experimental Measurements from the Los Alamos Free-Electron Laser Oscillator Experiment," Nucl. Instr. and Meth. in Phys. Res. A250, 4-11 (1986).

[18] M. T. Lynch, R. W. Warren, and P. J. Tallerico, "The Effects of Linear-Accelerator Noise on the Los Alamos Free-Electron Laser," IEEE J. Quant. Electron. 21 (7), 904-908 (1985).

[19] W. E. Stein, R. W. Warren, J. C. Winston, J. S. Fraser, and L. M. Young, "The Accelerator for the Los Alamos Free-Electron Laser-IV," IEEE J.Quant. Electron. 21 (7), 889-894 (1985).

[20] R. L. Sheffield, W. E. Stein, R. W. Warren, J. S. Fraser, and A. H. Lumpkin, "Electron Beam Diagnostics and Results for the Los Alamos Free-Electron Laser," IEEE J. Quant. Electron 21 (7), 895-903 (1085).

[21] D. W. Feldman, R. W. Warren, B. E. Carlsten, W. E. Stein, A. H. Lumpkin, S. C. Bender, G. Spalek, J. M. Watson, L. M. Young, J. S. Fraser, J. C. Goldstein, H. Takeda, T. S. Wang, K. C. D. Chan, B. D. McVey, B. E. Newnam, R. A. Lohsen, R. B. Feldman, R. K. Cooper, W. J. Johnson, and C. A. Brau, "Recent Results from the Los Alamos Free-Electron Laser," to be published IEEE J. Quant. Electron, special issue on free-electron lasers, 1987.

[22] B. E. Carlsten, D. W. Feldman, A. H. Lumpkin, W. E. Stein, J. E. Sollid, and R. W. Warren, "Emittance Studies of the Los Alamos National Laboratory Free-Electron Laser," these proceedings.

FIGURE CAPTIONS

Fig. 1. Shape of optical micropulse for standard conditions after different number of passes. The leading edge of the pulse is on the right side. A) 25 passes, B) 75 passes, C) 125 passes, and D) 200 passes.

Fig. 2. Spectra of the optical pulses presented in fig. 1.

Fig. 3. Extraction efficiency vs pass number for standard conditions and zero detuning. Curve A results when an ideal optical filter is inserted inside the cavity.

Fig. 4. Extraction efficiency vs pass number for conditions different from fig. 3. Curve A uses an optical filter with a cutoff spaced a few percent to longer wavelengths than the main line. Curve B has no filter.

Fig. 5. Extraction efficiency vs detuning for standard conditions. Shown are the efficiencies measured at the early plateau and the final plateau. The region where chirp and sidebands are observed is shaded. Point A corresponds to the detuning often used.

Fig. 6. A series of pulse shapes illustrating the sliding of the modulation off the leading edge with adequate detuning. A) modulated pulse before detuning, B) modulation at pass 625, C) modulation at pass 650, and D) modulation gone at pass 700.

Fig. 7. Spectra of the pulse shapes shown in fig. 6.

Fig. 8. Comparison of simulation of detuning curve with experimental data.

Fig. 9. Pulse shapes during 217-pass cycle where timing of micropulses is varied sinusoidally by ± 4ps . A) pass 500, B) 525, C) 550, D) 575, E) 600, F) 625, G) 650, and H) 675.

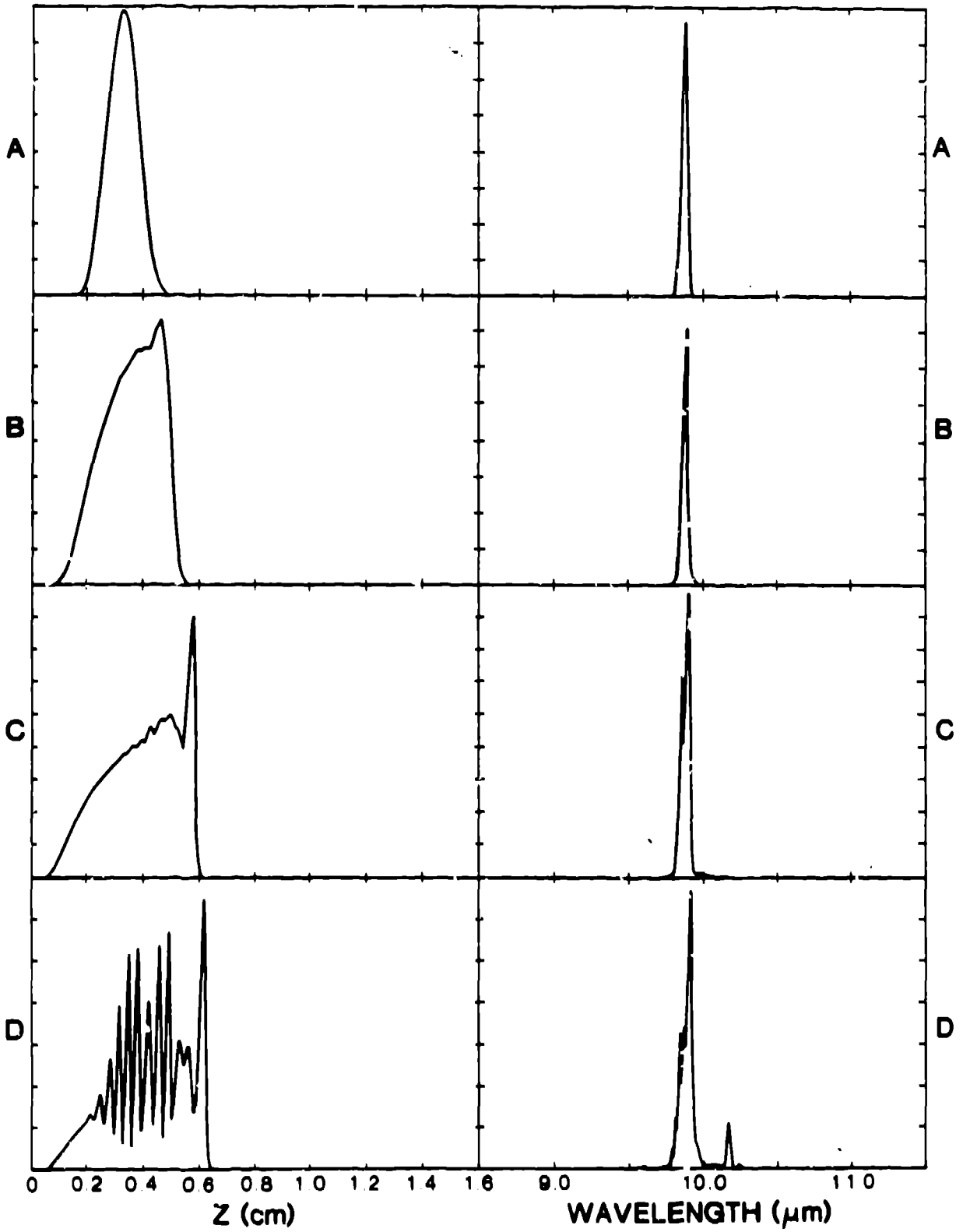
A
B
C
D
A
B
C
D
0
0.2
0.4
0.6
0.8
1.0
1.2
1.4
1.6
Z (cm)
9.0
10.0
11.0
WAVELENGTH (μm)

Mask out these words

SATURATION SHOWS EARLY P

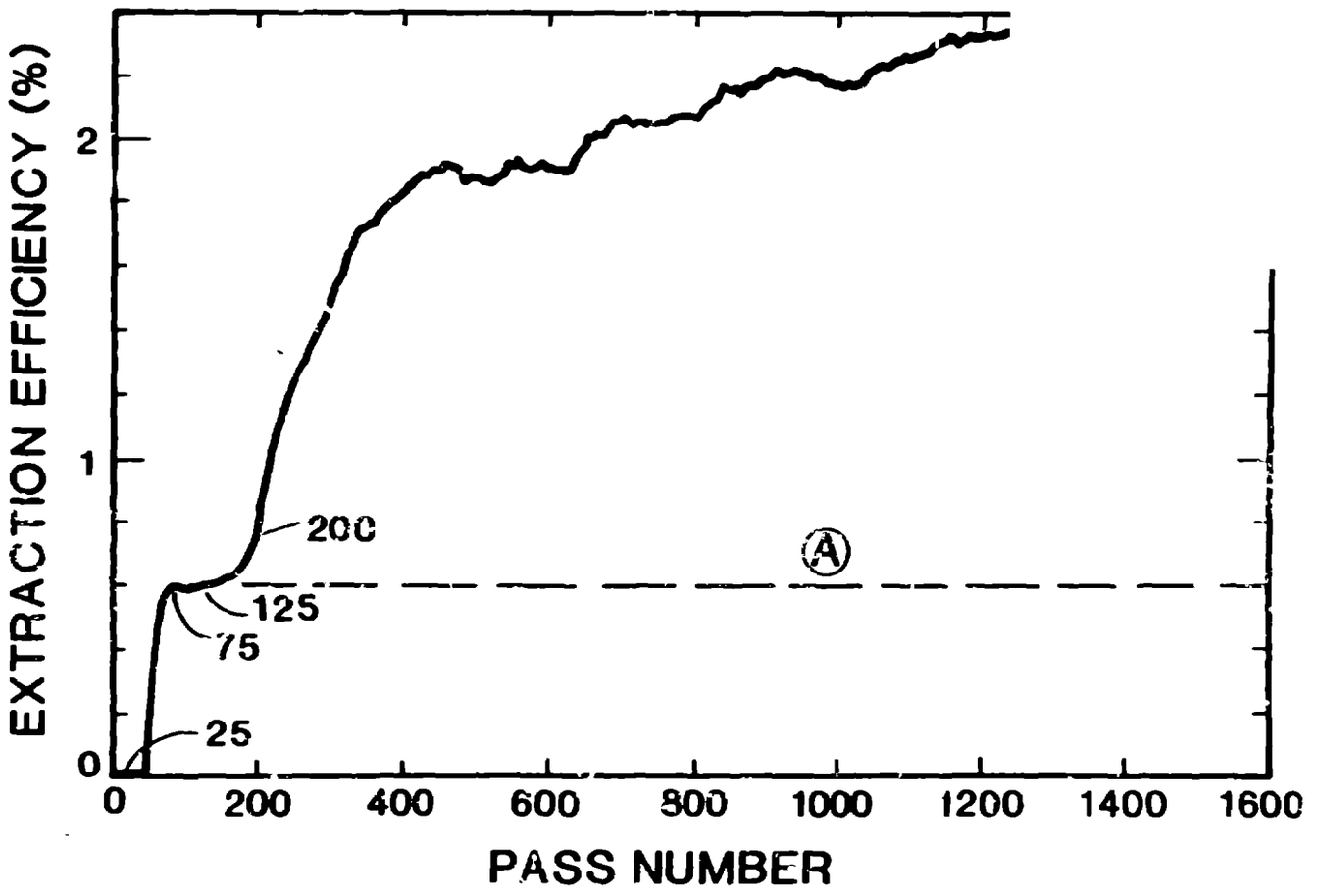

Make out - these words

SATURATION WITH GRATING OC(
LOW POWER

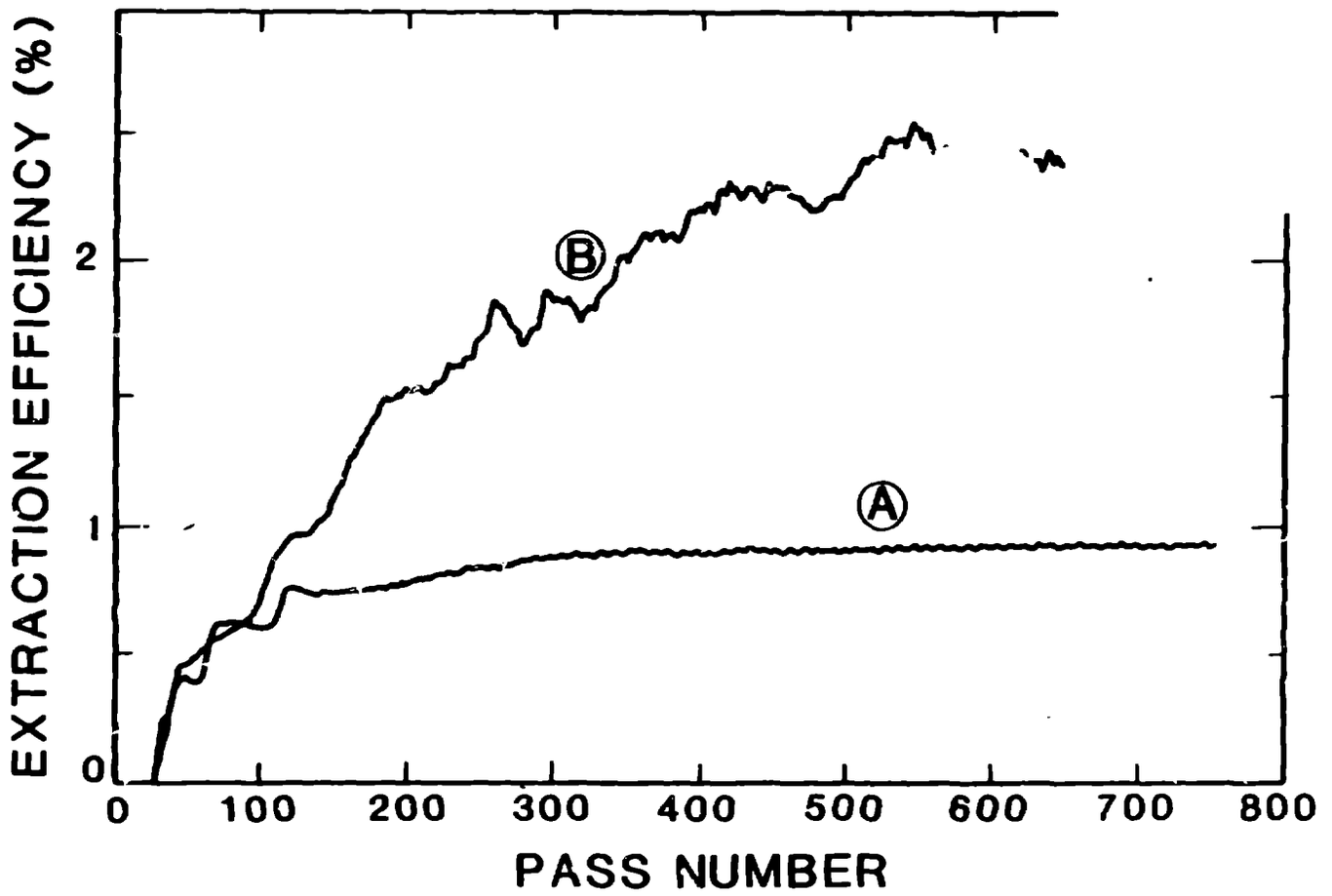

EARLY AND FINAL SATURATIOI
ONLY IN CHIRP REGIOI

Mask out these words

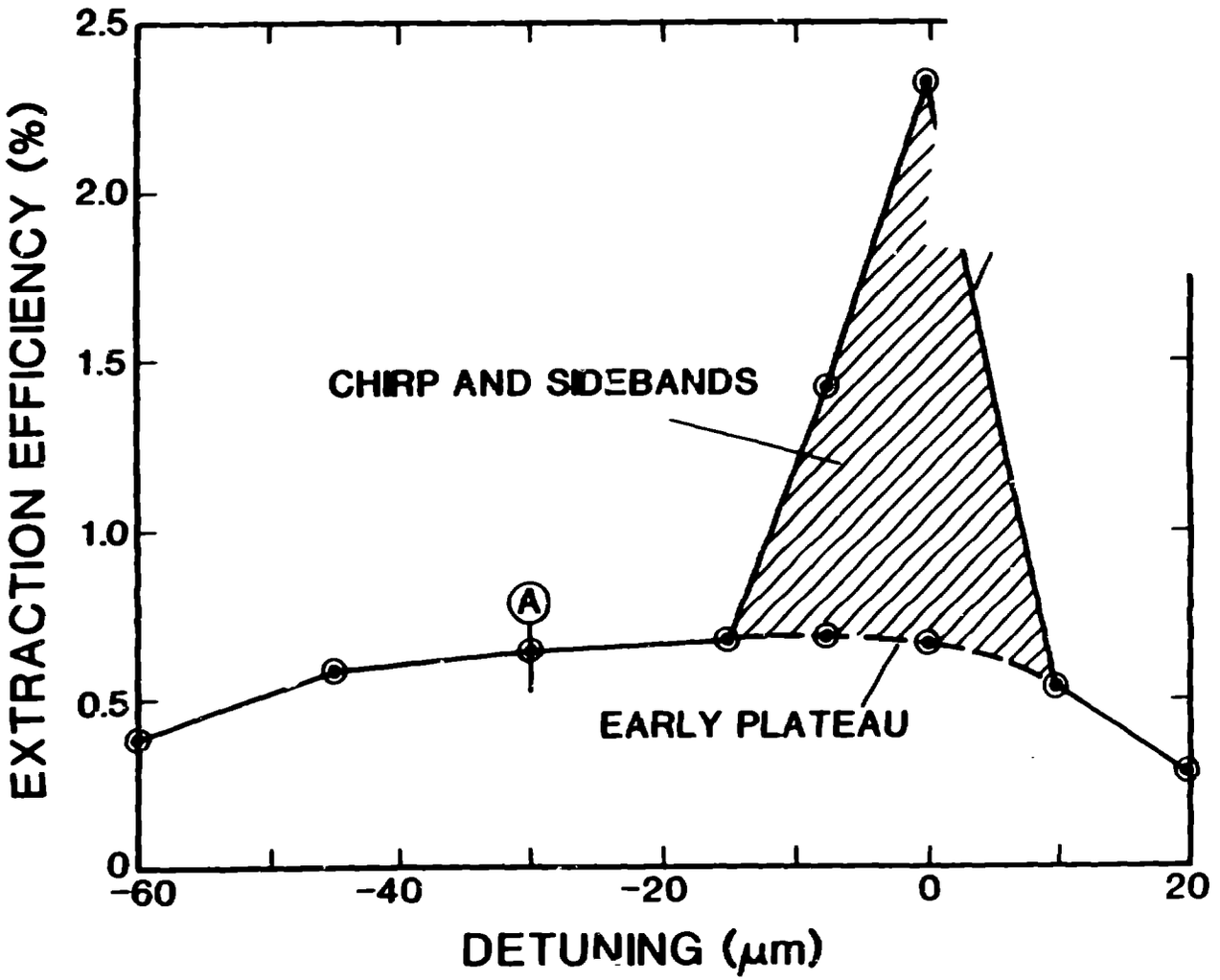

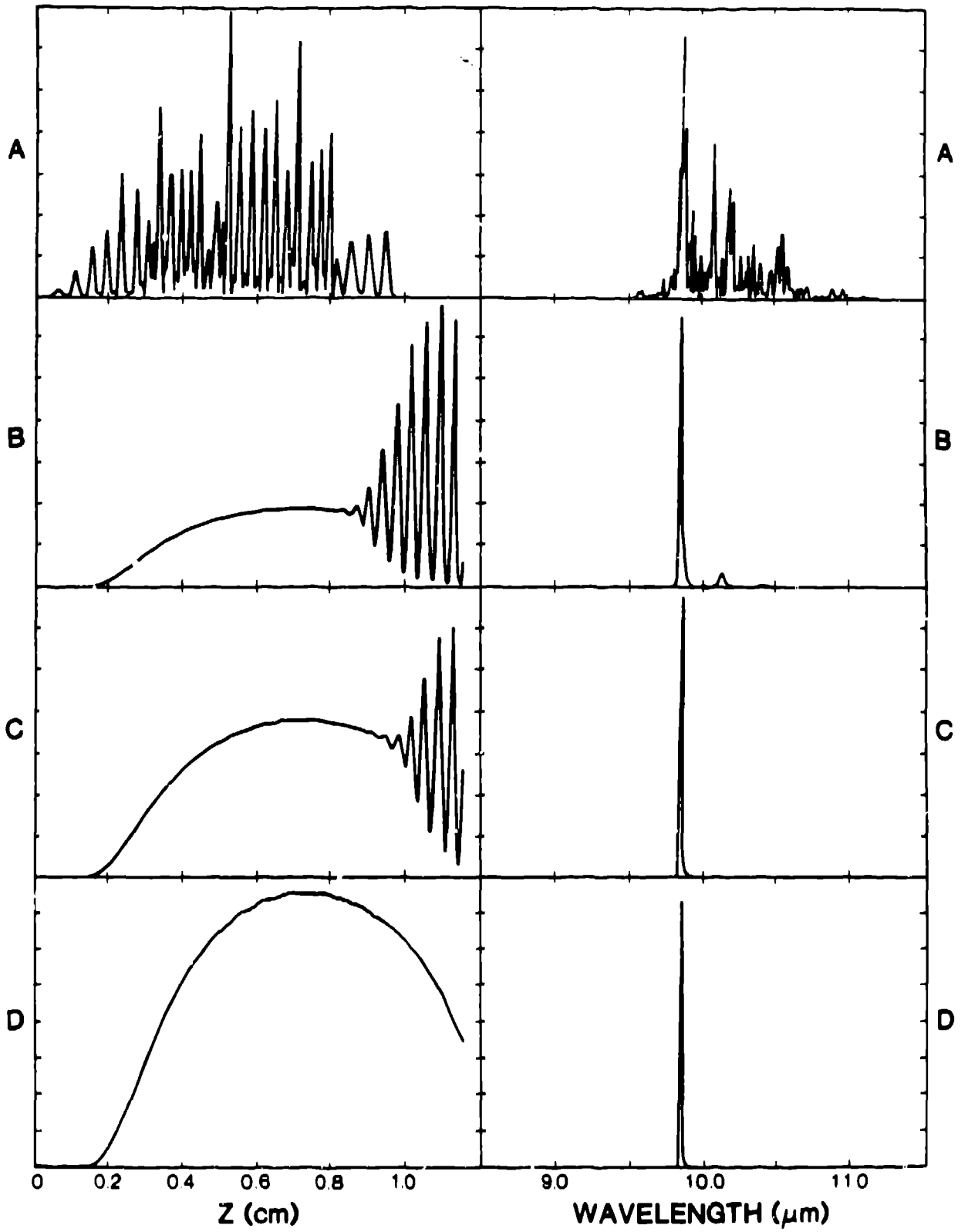
A
B
C
D
A
B
C
D
0
0.2
0.4
0.6
0.8
1.0
Z (cm)
9.0
10.0
11.0
WAVELENGTH (μm)

MEASURED AND CAL
DESYNCHRONISM CURVI

Mark out-there words

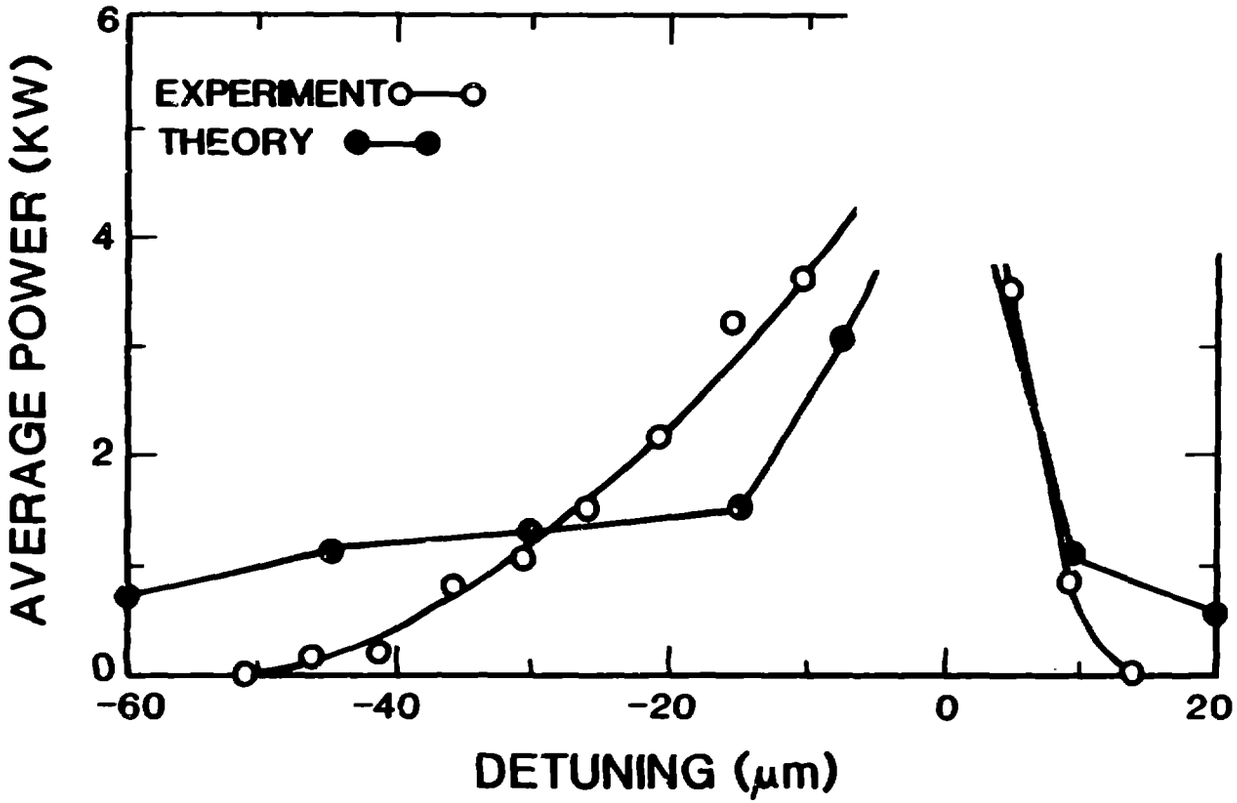

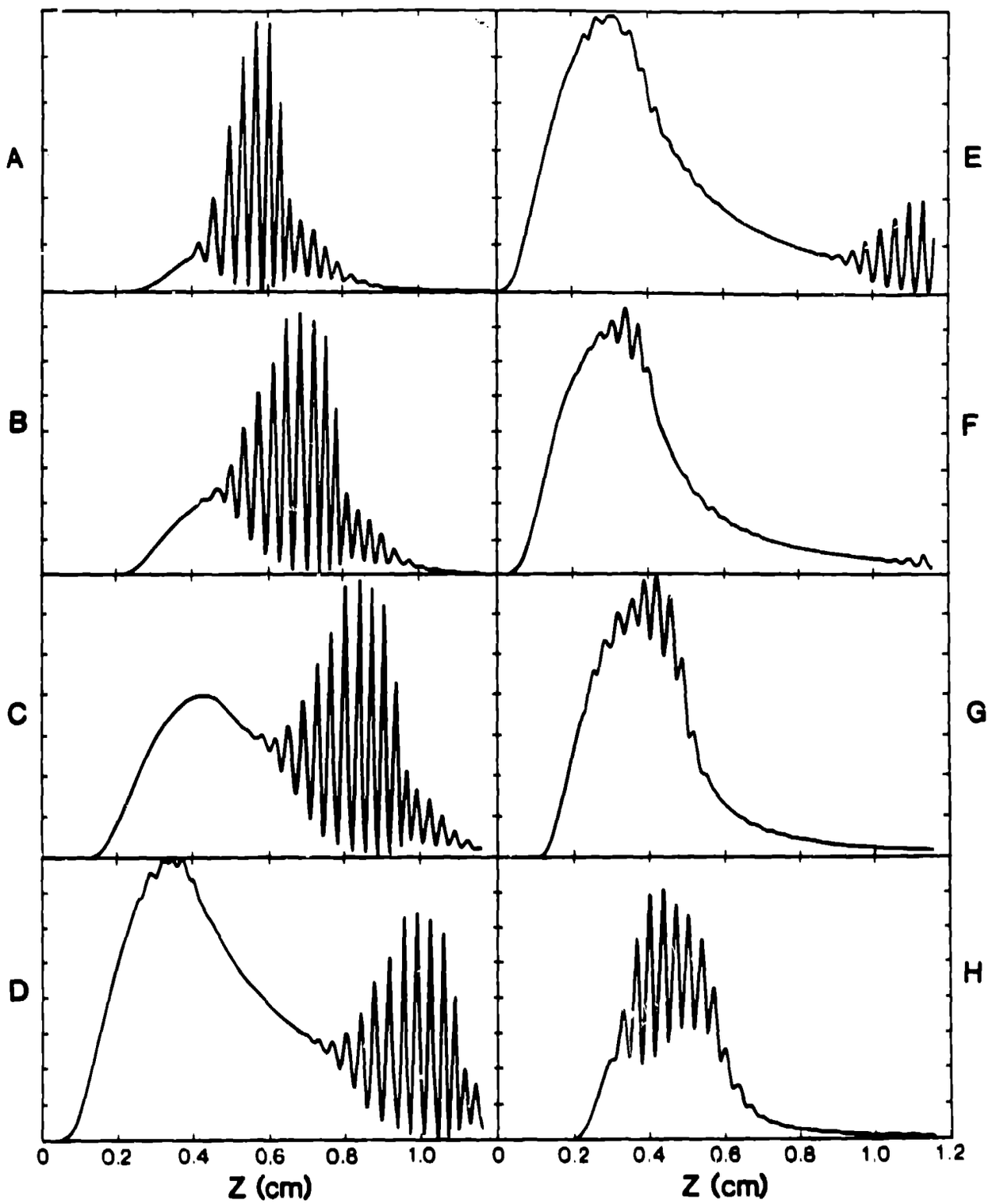
A
B
C
D
E
F
G
H
0
0.2
0.4
0.6
0.8
1.0
1.2
Z (cm)
Z (cm)